Examining Solute-Solvent Interactions at the Electrode Double Layer by Impedance Measurements of Proteins: 2. Prothrombin

C.V. Krishnan[1,2] and Merrill Garnett[1]*

[1]Garnett McKeen Lab, Inc., 7 Shirley Street, Bohemia, NY 11716-1735, USA
[2]Department of Chemistry, State University of New York, Stony Brook, NY 11794-3400, USA
[*]E-mail: ckrishnan@notes.cc.sunysb.edu ; tel. +6315890770; fax +6315890778

The electrochemical behavior of prothrombin (blood coagulation Factor II) from bovine plasma, studied by using cyclic voltammetry, indicate that this protein is strongly adsorbed on the mercury electrode and the adsorption increases with increasing concentration. The adsorption behavior is different on interaction with NaCl. The admittance increases in the frequency range 5000 to 250 Hz and then decreases with further decrease in frequency in the potential range -0.5 to -0.1 V. As the potential is increased further and changes sign, the admittance increases and goes through a maximum in the low frequency region. There is a shift in the maximum in admittance to still more positive (or less negative) potentials at lower frequencies and is attributed to the water structure breaking and orientation effects of water at the double layer. The admittance behavior is nearly the same in the presence of NaCl. However the decrease in admittance starts at a higher frequency than in the absence of NaCl. For prothrombin, the impedance shows unique impedance loci in the first two quadrants at 0.32-0.38 V. The negative differential resistance is attributed to the oscillatory behavior of the system, which is probably a characteristic of biological systems that self-assemble. The impedance locus in the second quadrant indicates two processes and may be associated with energy transfer involving the two kringles in the prothrombin structure. NaCl impedes the observed oscillatory phenomenon and consequently the negative differential resistance. Lower concentrations of prothrombin promote chaotic phenomena, the last stage of oscillations. The capacitance data show dispersion with frequency. Two capacitance minima observed in the cathodic region exhibit potential shifts depending on frequency. Mott-Schottky plots indicate both p-type and n-type semiconduction. The phase microscopy indicates unique concentration dependent self-assembly in the presence and absence of NaCl.

1. INTRODUCTION

We are interested in understanding the interactions of water on biological surfaces for signaling purposes. Water molecules are often involved in protein-DNA recognition [1]. The role of hydrogen bonding, C-H….O hydrogen bonds, as well as water mediated contacts between protein and DNA have been explored in understanding their interaction. The role of water in protein structure, molecular recognition, and catalysis are also extensively reviewed [2]. The structure and dynamics of water surrounding biomolecules have also been investigated [3] with special reference to cooperativity in cyclic motifs, hydrogen bonding flip-flop dynamics, and three center hydrogen bonds involved in sliding water along the surfaces of macromolecules.

Since all the biochemical processes take place in a milieu of aqueous electrolytes one should not overlook their importance. The morphology of the small water networks attached to halide ions, the importance of charge-transfer in the binary interaction, formation of negatively charged water clusters, $(H_2O)_n^-$, and the interaction of diffuse excess electrons with the water networks have recently been reviewed [4]. Stable hydrogen bonded networks of water with transfer of protons along the hydrogen bonds [5] have been attributed to the high proton mobility in ice as well as in protein crystals. Parallel explanations for electron transfer with tunneling of electrons in ice have been proposed [5]. Monte Carlo study of water near a charged surface has indicated a sense of "freezing" of water into a rigid ice like structure [6]. Additional complexities might arise when we realize that there are seven interfacial connectivities for a water molecule [7]. Also recent experiments have confirmed the existence of electrons on the surface as well as inside the water molecule depending on the size of the water cluster [8].

We are not aware of any data related to the behavior of water molecules on surfaces of biological molecules at low frequencies. We have found recently that impedance is a powerful technique to gather information about the nature of water molecules on the surfaces of biological molecules as well as electrolyte behavior in the double layer. Our frequency response analysis results on palladium-lipoic acid complex [9-10] as well as DNA with and without alkali halides and hydrogen peroxide [11-13] prompted us to look further into the self-assembly properties of other biological molecules that may be involved in electronic signaling. Prothrombin is heavily studied for its crystal structure and function [14] due to its importance in the blood clotting cascade process. Prothrombin regulation is essential to control bleeding as well as thrombosis because of its dual role in both the coagulation and anticoagulation of blood. Earlier we have studied the interaction of prothrombin with hyaluronic acid, and magnetic fields [15], and have spun fibers of prothrombin-hyaluronic acid at the mercury electrode [16].

A complex cascade of reactions are involved in blood coagulation. These reactions rapidly amplify an initiation stimulus and lead to generate blood clots. Prothrombin is the precursor to thrombin in this cascade process. The goal of the coagulation cascade is for the thrombin to convert fibrinogen into fibrin.

Thrombin in humans has two disulfide-linked polypeptide chains [14]: a 36-residue A chain and a 259-residue B-chain. It is synthesized as a 579-residue zymogen prothrombin (II). The two polypeptide bonds are cleaved by Stuart factor X_a. The activation of prothrombin by the factor X_a is enhanced by

the combination of negatively charged phospholipids and calcium ions [17]. The separation of the A and B chains and release of the N-terminal propeptide are achieved by cleavage of Arginine 271-Threonine 272 and Arginine 320-Isoleucine321 bonds.

The prothrombin gene mutation was first described as a genetically acquired trait in 1996. The mutation in the position 20210 increases the concentration of thrombin circulation in the blood stream and leads to deep venous thrombosis and probably to arterial thrombosis causing stroke or heart attack.

Our particular interest in this study comes from the peculiar structure of prothrombin's propeptide. Its three domains consist of a 40-residue γ-carboxyglutamate (Gla) domain and two other 40% identical, and approximately 115-residue "kringle" domains. Three disulfide bonds cross-link each of these kringles. These triple-looped motifs have a folded appearance due to the cross-linking. Since these kinds of domains and kringles are characteristic of several proteins involved in the formation and breakdown of blood clots, we became interested in investigating the role of water and its frequency dependent behavior. By comparing this study with that of thrombin, one can obtain information regarding the domain containing the kringles.

2. EXPERIMENTAL PART

2.1 Materials

Prothrombin from bovine plasma was from ICN Biochemicals Inc., (Cat. No. 101033), with an activity of 122 units/mg protein and activity of 50 units/mg solid. The molecular mass of purified prothrombin is 68000-68500. The NaCl used was Analytical grade. Distilled water was used for preparation of all solutions.

2.2. Methods

An EG & G PARC Model 303A SMDE tri electrode system (platinum counter electrode and Ag/AgCl (saturated KCl) reference electrode) along with Autolab eco chemie was used for cyclic voltammetric and electrochemical impedance measurements at 298 K. The solutions were carefully purged (because of foaming problems) with N_2 for about 10 minutes before the experiment. Impedance measurements were carried out using about 7 mL solutions in the frequency range 5,000 Hz to 10 mHz. The amplitude of the sinusoidal perturbation signal was 10 mV. Even though it is known that glass activates Hageman factor (Factor XII) and probably activates prothrombin [18], we have done experiments using glass cells only.

3. RESULTS AND DISCUSSION

3.1. Cyclic Voltammetry

These measurements were made for 25 mg/mL prothrombin in the presence and absence of 0.005 M and 0.10M NaCl, 10 and 2.5 mg/mL prothrombin in the presence and absence of 0.10 M NaCl at a scan rate of 100 mV/s, by scanning in three potential regions. The first region, 0.0 to -1.0 and back to 0.0 V, falls within the conventional range of the mercury working electrode. In the second range, 0.3 to –1.0 and back to 0.3V, the mercury is slightly passivated and the chloride begins to interact. In the third widest range, 1.0 to –1.0 and back to 1.0 V, mercury is completely passivated and the chloride

interacts strongly. The idea behind scanning through this wide region is to encompass natural biological surfaces with both positive and negative charges. Thrombosis, which involves intermediate steps of electrochemical origin, is the major cause of heart attack due to the formation of solid or semisolid mass from the various constituents of blood within the heart or blood vessels. It is known that thrombosis is initiated by positively charged surfaces and inhibited by negatively charged surfaces [18]. We chose the mercury electrode because we understand its polarization range. Of course there is the ease with which we can get fresh electrode surfaces by using a new drop each time. Three scans were made for each potential region. For different concentrations of prothrombin, the results for the scans in the third range of +1.0 to –1.0 and back to +1.0V are shown in Figure 1a. We wish to point out that for 25 mg/mL pure prothrombin, cathodic peaks at 0.080, –0.276, and –0.418 V are observed for the scans in the three ranges. Also a small hump or shoulder is observed at 0.539 V for the scan in the widest range. An anodic peak at 0.551 was observed only for the scan in the third range. Figure 1a
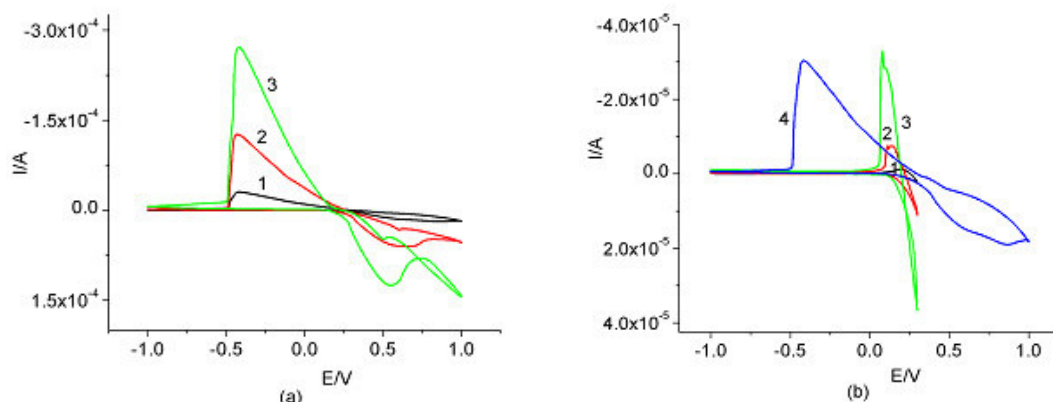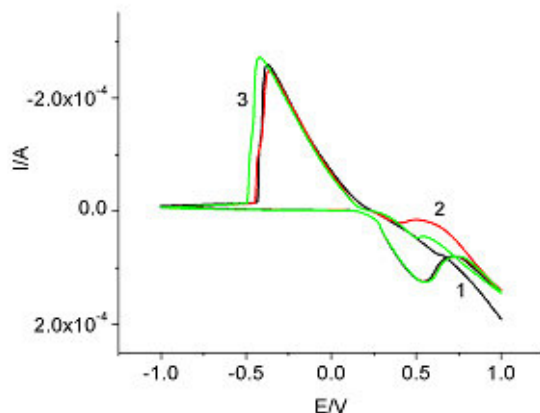

Figure 1. Cyclic voltammetry of prothrombin from bovine plasma pH 6.55-6.88 a) scan range 1.0 to –1.0 and back to 1.0 V; 1, 2.5 mg/mL; 2, 10 mg/mL and 3, 25 mg/mL; b) scan range 0.3 to –1.0 and back to 0.3 V; 1, 2.5 mg/mL; 2, 10 mg/mL; 3, 25 mg/mL. For comparison the data for 2.5mg/mL in the scan range 1.0 to –1.0 and back to 1.0V are included as curve 4.

also shows that the adsorption increases with increasing concentration of prothrombin. Figure 1b shows the data for 2.5, 10 and 25 mg/mL prothrombin in the second scan range 0.3 to –1.0 and back to 0.3 V. It is clear that there is comparatively much less adsorption when the scan is restricted to much less anodic potentials. Also the peaks are less broad. To compare the shift in potentials, Figure 1b also shows the data for 2.5 mg/mL prothrombin for the scan in the widest range.

The results for three consecutive scans are shown in Figure 2. It is obvious that there are very minor changes only with change in the number of scans. We have not carried out continuous cycling in order to look for the appearance of new peaks as observed previously [18].

The cyclic voltammograms of 25 mg/mL prothrombin in the presence of NaCl are shown in Figure 3a. In the presence of 0.005 M NaCl, there was no cathodic peak for the scan in the first range, with 0.027 and –0.155 V for the scans in the other two ranges. A post-cathodic peak or hump is also observed at –0.24 V. The anodic peak was at 0.485 V. The presence of NaCl shifts the cathodic peaks to less negative potentials and the anodic peaks to less positive potentials. The peak also becomes sharper in the presence of NaCl. Both the cathodic and anodic peak currents are much higher than the

NaCl blank alone indicating strong adsorption in the presence of NaCl. However this is different from that observed without any NaCl. The curve with 0.005 M NaCl is in between that with 0.10 M NaCl and no NaCl.

Figure 2. Cyclic voltammetry of prothrombin from bovine plasma, pH 6.88 in the scan range 1.0 to – 1.0 and back to 1.0 V (a) 25 mg/mL; 1, scan 1; 2,scan 2; 3,scan 3
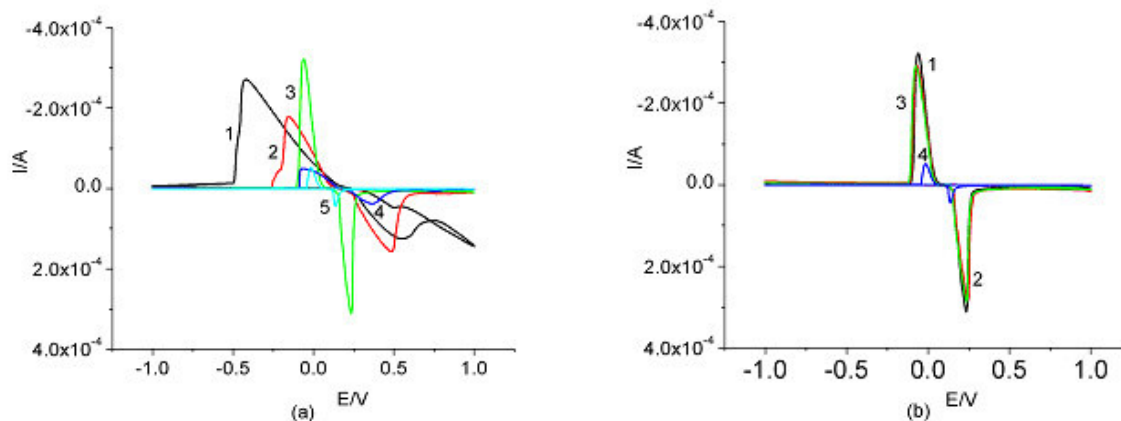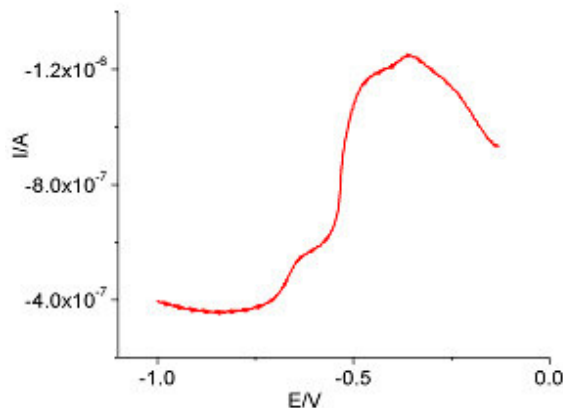

Figure 3. Cyclic voltammetry of prothrombin from bovine plasma, pH 6.16-6.88 in the scan range 1.0 to −1.0 and back to 1.0 V (a) 25 mg/mL; 1, no NaCl; 2, in 0.005 M NaCl; 3, in 0.10 M NaCl; 4, 0.005 M NaCl blank; 5, 0.10 M NaCl blank; (b) Prothrombin concentration dependence in 0.10 M NaCl; 1, 25 mg/mL; 2, 10 mg/mL; 3, 2.5 mg/mL; 4, NaCl blank

The data for prothrombin concentration in the presence of 0.10 M NaCl are compared in Figure 3b. The strong interaction of NaCl with prothrombin is obvious from these curves when compared to that of the blank NaCl. The differences are negligible with respect to the prothrombin concentration. With 0.10 M NaCl we have observed nearly the same current and peak position irrespective of the amount of prothrombin. We have also observed that both the cathodic and anodic currents are much less for the NaCl blank.

Figure 4 shows the expanded plot in the region -1.0 to -0.13V of curve 3 in Figure 3a, 25 mg/mL prothrombin in 0.10 M NaCl. This shows that Figure 3b is somewhat deceiving because of the high

current and that there is still some adsorption of prothrombin in the region observed in the absence of NaCl. However the current is about 100 times smaller than the amount observed for prothrombin alone.

The results in Figures 1-4 are in accordance with the characteristics of adsorption process. When

Figure 4. Cyclic voltammetry of 25 mg/mL prothrombin in 0.10 M NaCl in the scan region
-1.0 to -0.13 V.

there is strong adsorption, a post-wave or post-peak is often observed [19]. This contributes to higher cathodic currents. In the case of weak adsorption no post-peak is observed, but only an increase in cathodic current.

Earlier studies of cyclic voltammetry of prothrombin (0.1 and 1 unit/mL) show that it is adsorbed at lower concentrations and undergoes charge transfer reaction at higher concentrations at the platinum electrode in 0.154 M sodium chloride [18,20]. Compared to this, our highest concentration of prothrombin is 25 mg/mL or 1250 units/mL and the lowest concentration is 125 units/mL. In the earlier study [18] it was established that the species participating in the electrode reaction at negative potentials is the product of the reaction prothrombin undergoes in the positive potential region, where the possibility of an intermediate is considered. Comparison of our data in Figure 1a and Figure 1b also suggests the possibility of an intermediate species. We must point out that in the studies with human prothrombin, the cyclic voltammograms were identical to those of the blank 0.15 M NaCl [20] and different from the observations with prothrombin from bovine plasma [18].
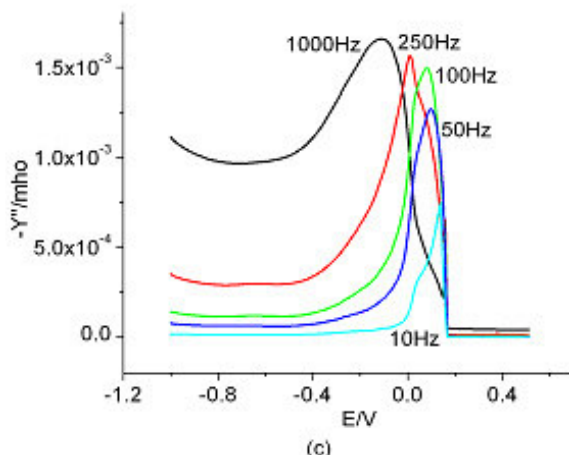
3.2. Admittance

Our admittance results for 25 mg/mL prothrombin in the absence and presence of 0.005M NaCl are shown at different frequencies in Figure 5a, b. The admittance increases with decreasing frequencies up to about 250Hz and then decreases at lower frequencies. However at lower frequencies the admittance increases with increasing potential. This is attributed to changes in the orientation of water molecules as the double layer re-configures at potentials close to zero. When the potential changes from negative to positive, the orientation of water molecules changes from the hydrogen to the oxygen oriented towards mercury. Also there must be orientation changes in the protein charge pointing

towards mercury. Judging by the admittance results at low frequencies, water structure- breaking must be dominant in this process, contributing to an increase in admittance.
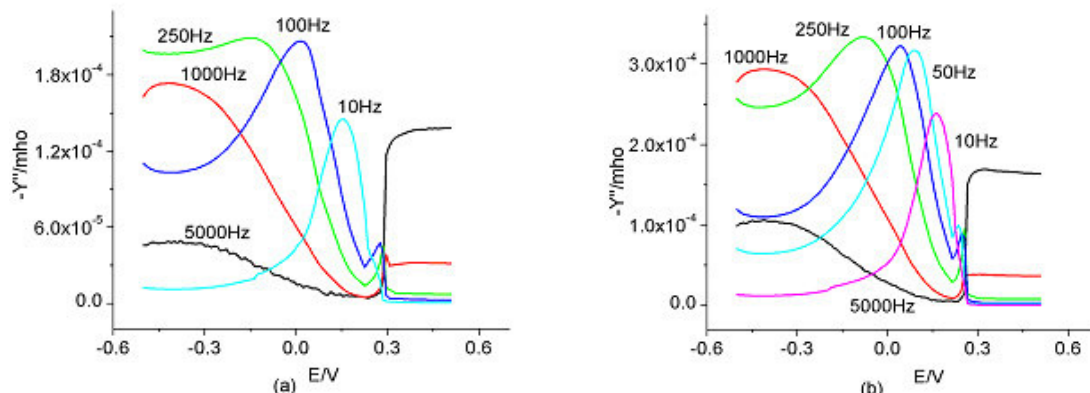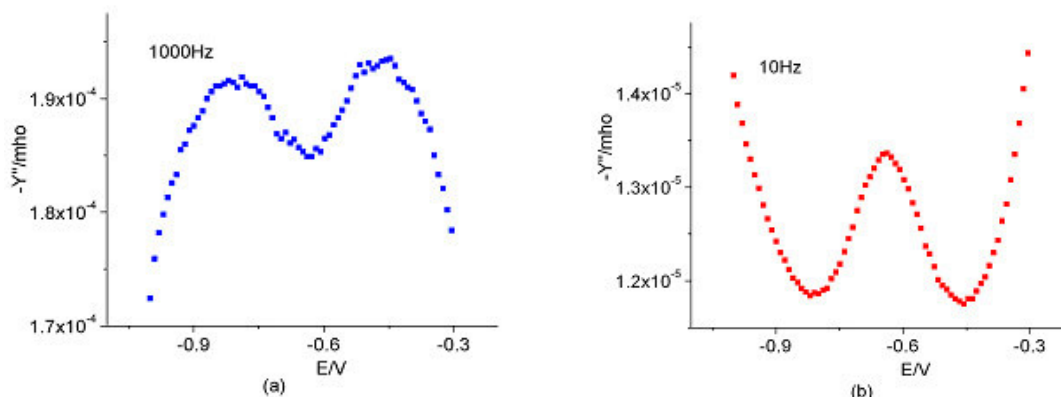

Figure 5a,b. Admittance of a) 25 mg/mL prothrombin from bovine plasma, pH 6.88 b) 25 mg/mL prothrombin in 0.005 M NaCl, pH 6.79

The admittance results with 25mg/mL prothrombin in 0.10M NaCl are shown in Figure 5c. The

Figure 5c. Admittance of 25 mg/mL prothrombin from bovine plasma in 0.10 M NaCl and pH 6.16 at 1000, 250, 100, 50 and 10 Hz.

results are mostly similar in behavior to that observed in Figure 5b. We have observed similar admittance behavior for aqueous solutions of alkali chlorides. In this Figure 5c we have used the scan in the range of -1.0 to 0.5 V in order to get the results of adsorption at more cathodic potentials. The dominance of admittance values close to 0.0 V masks the effects in more cathodic potentials. This is seen more clearly in Figure 6a,b and is also discussed in more detail in Section 3.5. The behavior observed at 1000Hz is different from the behavior at frequencies of 100Hz and lower. We observe two maxima around -0.80 and -0.48V at 1000 Hz compared to the two minima around the same potentials at lower frequencies. Similar behavior is also observed when the results of Figure 5c for 25mg/mL prothrombin in 0.10M NaCl are plotted in an expanded window.

Figure 6. Admittance in the expanded window for 25 mg/mL prothrombin from bovine plasma, pH 6.88 at a) 1000Hz; b)10 Hz

Due to larger thermal vibrations displayed by peripheral amino-acid side chains, the water around them exhibits even more thermal vibrations and these form "soft" hydrogen bonds [3]. When several O-H ….O-H ….O-H bonds all run in the same direction, the homodromic arrangement contributes to additional stability. Entropy preferred three center (bifurcated) hydrogen bonds with "flip-flop" dynamics are favored for the movement of water along the surface of macromolecules [3]. This facilitates configuration changes smoothly. Macromolecules also seem to favor pentagonal motifs of water molecules. Prothrombin is likely to exhibit this "flip-flop" dynamics. We are tempted at this time to attribute the "kringle" structure of prothrombin to the unusual and highly symmetric nature of the graphs in Figure 6. We have observed similar but less dramatic curves for collagen and is attributed to the orientation changes of water around the peptide groups when the potential gradually changes to less negative values.

3.3. Impedance

### 3.3.1. Nyquist and Bode plots

We have carried out the impedance at measurements at -1.0, -0.6, -0.3, 0.0, 0.1, 0.2, 0.3, 0.4, 0.5 and 0.6 V for 25 and 10 mg/mL prothrombin. The data could be fitted with R1(R2C1)(R3C2)(R4C3) at -1.0, -0.6, and -0.3 V, with R1(R2C1)(R3C2) at 0.0 and 0.1 V, and with R1(R2C1)(R3C2)(R4C3)(R5C4) at 0.2 V. The Nyquist and Bode plots for 0.2 V are shown in Figure 7a,b. The line shows the fits with
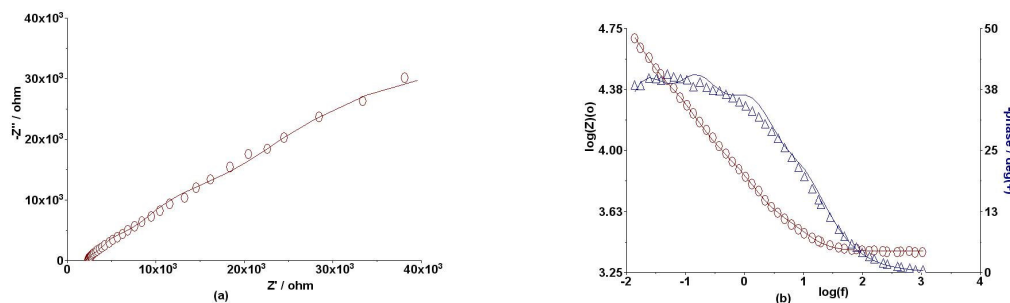
Figure 7a,b. Prothrombin, 25 mg/mL, pH 6.88, 0.2 V a) Nyquist plot, b) Bode plot. The equivalent circuit used to fit the data is R1(R2C1)(R3C2)(R4C3)(R5C4)

the circuit R1(R2C1)(R3C2)(R4C3)(R5C4). For all normal electrolytes including NaCl the data could be fitted for potentials from -1.0 to 0.0 V with R1(R2C1) as expected. The data could be similarly fitted with 4 RC units for prothrombin in the presence of NaCl up to 0.2 V. This kind of fit fails at potentials more positive than 0.2V.

We did attempt to fit the data at positive potentials. Even though we do not understand the full biological significance of this circuit, we could get a fairly decent fit with circuit of the type R1(R2C1)(R3Q1)(R4W1) (the values used for the fit are R1 = 10.06 kΩ, R2 = 48.9 kΩ, C1 = 12.35 nF, R3 = 55.9 kΩ, Q1 Yo =0.9398 x 10^{-9} and n = 0.5972, R4 = -0.348 MΩ, and W1 = 0.319 x 10^{-5}) as shown in Figure 7c,d.
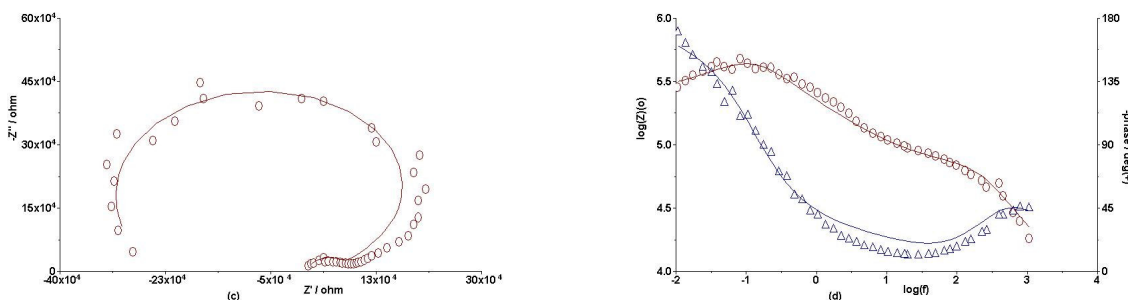
Figure 7c,d. Prothrombin, 25 mg/mL, pH 6.88, 0.36 V c) Nyquist plot, d) Bode plot. The equivalent circuit used to fit the data is R1(R2C1)(R3Q1)(R4W1)

3.3.2. Effect of anodic potential

We observed in our studies with palladium lipoic acid complex that the impedance loci in four quadrants are very sensitive to the potential, concentration, and pH. A change in potential by more than 10 mV produced significantly different impedance behavior. The Nyquist and Bode plots for 25 mg/mL prothrombin in the potential range 0.30 to 0.40 V are shown in Figure 8. The results are quite unique in that after the first small capacitive curve in the first quadrant, the impedance loci reverse direction and extend into the second quadrant. This phenomenon is classified as systems that exhibit negative differential resistance. The data are more consistent in the potential range 0.32 – 0.36 V. The data at the two ends of the potentials are more chaotic, even though they still exhibit negative
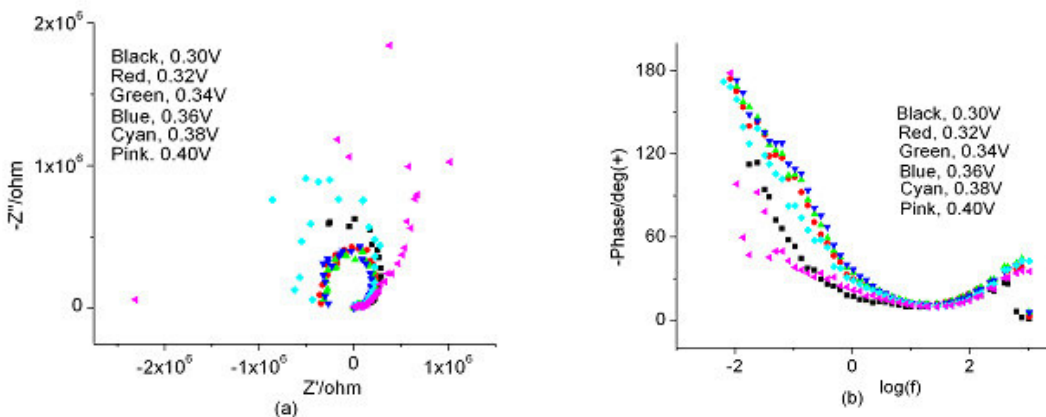
Figure 8a,b. Impedance data for 25 mg/mL prothrombin from bovine plasma, pH 6.88, 0.30 – 0.40 V. a) Nyquist plot b) Bode plot, phase

differential resistance convincingly.   The impedance behavior exhibiting negative differential resistance has a good tolerance of about 60 mV compared to the palladium lipoic acid system. The Bode plot also confirms the closeness of the data in the potential range 0.32 -0.36 V.
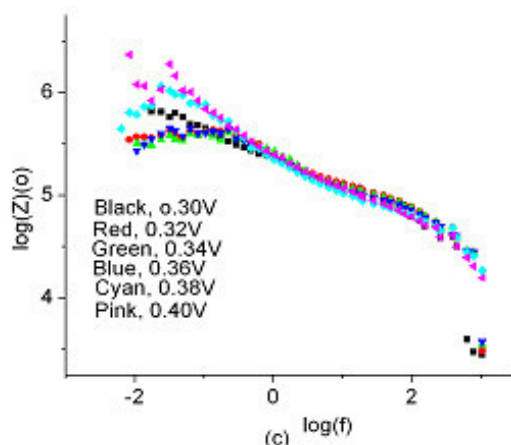
Figure 8c. Impedance data for 25 mg/mL prothrombin from bovine plasma, pH 6.88, 0.30 – 0.40 V; Bode plot, impedance modulus

3.3.3. Effect of concentration of prothrombin

In our early experiments with 2.5 mg/mL prothrombin we could not observe any impedance with negative differential resistance. However the indications from the results with this concentration and our past experience prompted us to look at higher concentrations and the results are shown in Figure 9. The results indicate that with higher concentrations, the impedance with negative differential resistance, becomes less and less. However there is not much difference in results for 15 to 25 mg/mL prothrombin. With 5 mg/mL prothrombin the results are chaotic, even though there is a definite trend for the negative Z'value. As mentioned before, we could not get any impedance loci in the second quadrant for 2.5 mg/mL prothrombin.
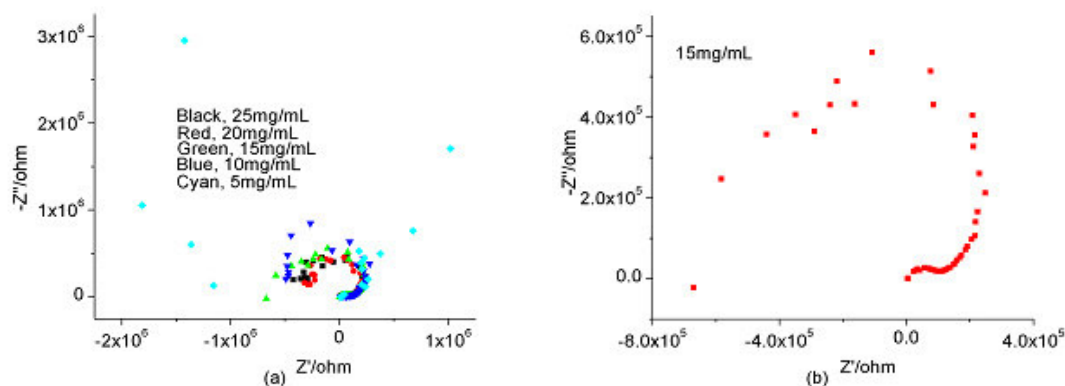

Figure 9. Concentration dependence of prothrombin from bovine plasma on negative differential resistance, pH 6.88, 0.36 V

In Figure 9b, the data for 15mg/mL prothrombin shown in Figure9a is replotted to highlight the nature of the curve. It does not look like a continuous smooth curve. It is too early to speculate the role of the two "kringles" in the prothrombin structure and its role in oscillatory phenomena or energy transfer between them.

3.3.4. Effect of surface area of the mercury drop

The influence of electrode surface area was determined by collecting impedance data at 0.36 V where negative differential resistance was observed. The results are shown in Figure 10. The numbers in the figure indicate the number of times the button has been pressed for increasing the size of the
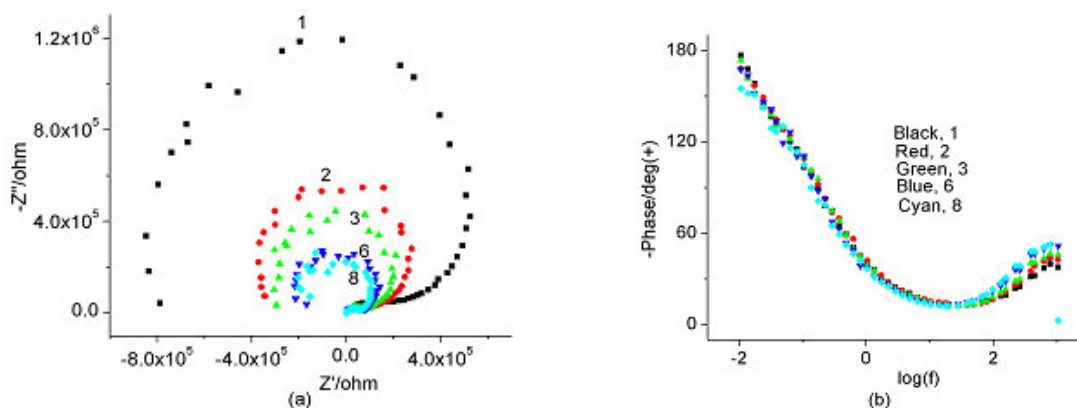
Figure 10a,b.   Impedance data for 25 mg/mL prothrombin from bovine plasma, pH 6.88, 0.36 V. The numbers in the figure, 1,2,3,6,8, indicate the number of times the button for controlling the size of the mercury drop has been pressed; a) Nyquist plot; b) Bode plot, phase

mercury drop. The model 303A SMDE system allows three drop sizes, small, medium, and large. We have carried out all our normal measurements using the small drop. In FRA measurements the drop size is determined by pushing the button 3 times. The surface area of the drop was determined using the push button and dislodge button for collecting 5 drops and finding the mass. The approximate surface area of the drops obtained by pushing the button 1, 2, 3, 6, and 8 times are 0.011, 0.017, 0.022, 0.035, and 0.042 cm^2. As the size of the mercury drop increases, the surface area increases and the overall size of the impedance plot decreases (Figure 10a). The change is most at the initial increase in the size of the drop, and finally the size effect becomes negligible with the large drops. The Bode plot in Figure 10b indicates practically no change in the phase as expected, but only in the modulus of the impedance as shown in Figure 10c.

We want to emphasize here that it is extremely difficult to do similar experiments with other working electrodes.

3.3.5. Stability

Quite often one raises the question about the reliability of these data. We have addressed this issue of the stability of the process and reproducibility of the data in three ways. Since we have used fresh

mercury drops each time, it is much easier to get an exactly reproducible surface compared to any other solid electrode. We have also checked the reproducibility in the normal range of the mercury
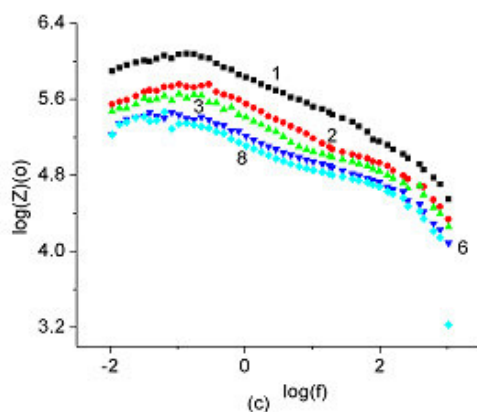
Figure 10c. Impedance data for 25 mg/mL prothrombin from bovine plasma, pH 6.88, 0.36 V. The numbers in the figure, 1,2,3,6,8, indicate the number of times the button for controlling the size of the mercury drop has been pressed; c) Bode plot, impedance modulus

working electrode as well as the partially passivated electrode at potentials where dramatic results in impedance are observed. Some typical results are shown in Figures 11-12. For the purpose of clarity
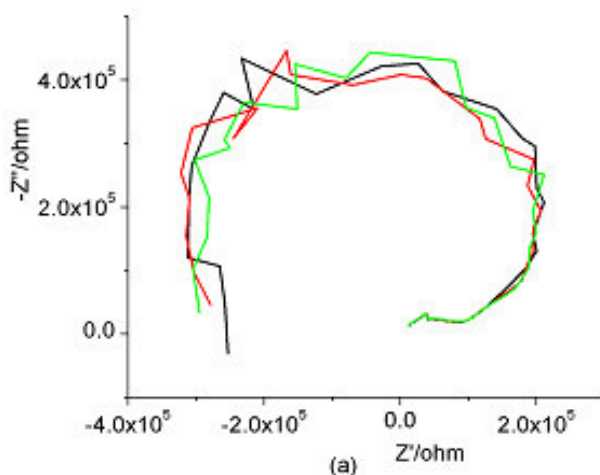

Figure 11a. Reproducibility of impedance data with negative differential resistance. 25 mg/mL prothrombin, pH 6.88, 0.36 V, three sets of data; Nyquist plot

three sets of data are shown in Figures 11 and 12. Both Nyquist and Bode plots as well as admittance and Mott-Schottky plots are shown to indicate that depending on the selection of the plot one may be tempted to draw different conclusions. We have repeated the experiments many times on the same day and sometimes after several months. The observed behavior is similar and reproducible. The figures do not warrant any deviations from the discussion we have presented so far. Since we have not used the data to calculate any rate data or to compute thermodynamic parameters, but only to suggest the nature of solute-solvent interactions, we have given more importance to the general trends in the curves rather

than to the absolute values. The data given in Figures 11-12 definitely reproduce the general trends. We assume that the self-assembly of the molecules in the solution provides a pathway for the spatial extension of the electrode. It is understandable to observe a small degree of variation in the results because the solution phase is purged each time before the experiment. This may slightly alter the arrangement of the self–assembly, each time, near the double layer.
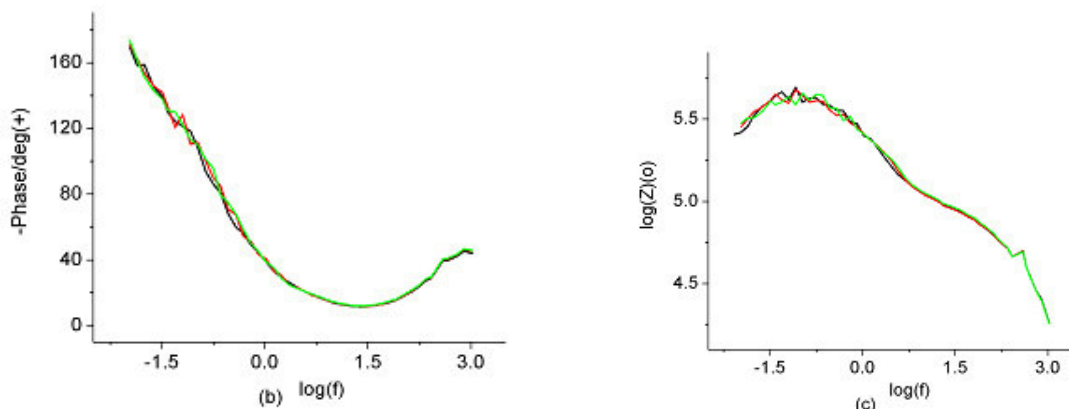
Figure 11b,c. Reproducibility of impedance data with negative differential resistance. 25 mg/mL prothrombin, pH 6.88, 0.36 V, three sets of data; Bode plots; b) phase c) impedance modulus
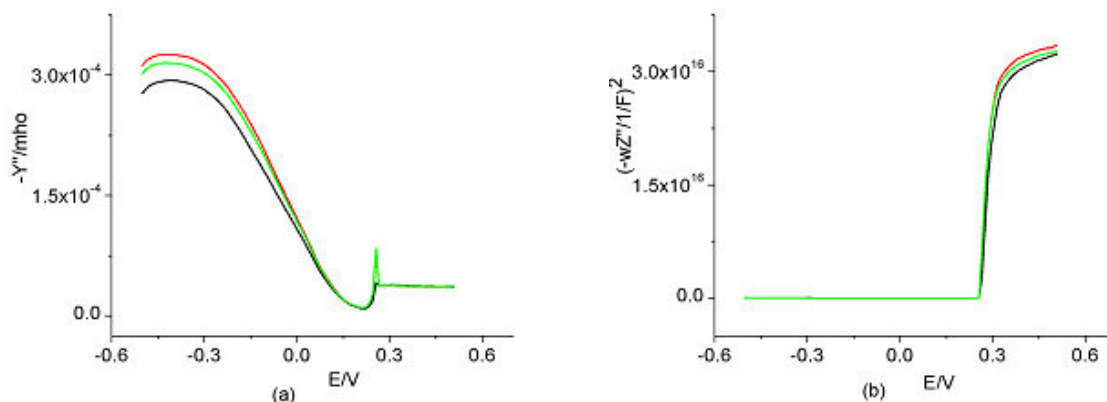

Figure 12. Reproducibility data for 25 mg/mL prothrombin in 0.005 M NaCl , pH 6.79, 1000 Hz, three sets of data; a) admittance b) Mott-Schottky plot

3.3.6. Effect of NaCl

The Nyquist and Bode plots at 0.38 V for 25 mg/mL prothrombin in the presence and absence of 0.005 M NaCl are shown in Figure 13. The data clearly demonstrate negative differential resistance that can tolerate small concentrations of NaCl. The Nyquist and Bode plots at 0.36 V for 25 mg/mL prothrombin in the presence and absence of 0.10 M NaCl are shown in Figure 14. This demonstrates that higher concentrations of NaCl impede the negative differential resistance and consequent resonant

tunneling or tunnel diode behavior. Thus the presence of the salt impedes the self-assembly or packing behavior which underlies the periodic changes in liquid crystal form (Figure19). These changes in form accompany the change in impedance direction. The change from branched to unbranched form is clearly an oscillation.
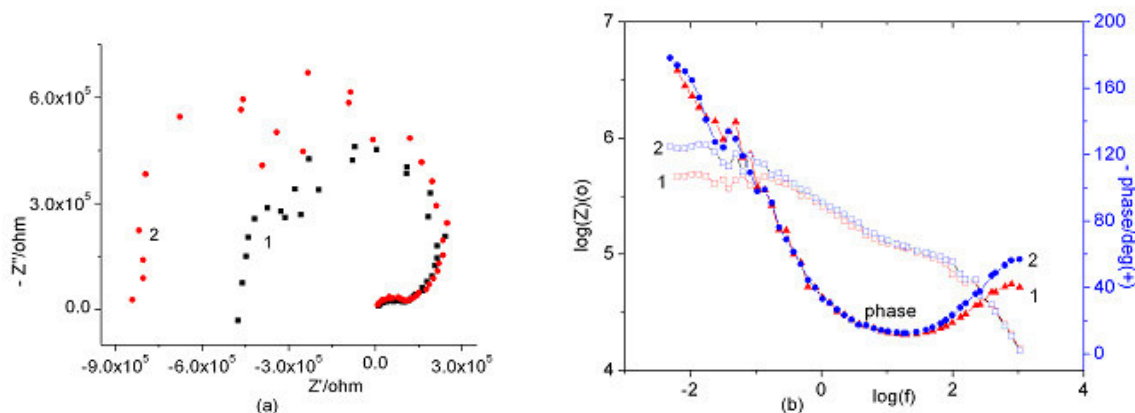
Figure 13. Impedance plots at 0.38 V, 1000 Hz – 5 mHz for a) Nyquist plot, 1, 25 mg/mL prothrombin; 2, 25 mg/mL prothrombin in 0.005 M NaCl; b) Bode plot, 1, 25 mg/mL prothrombin; 2, 25 mg/mL prothrombin in 0.005 M NaCl
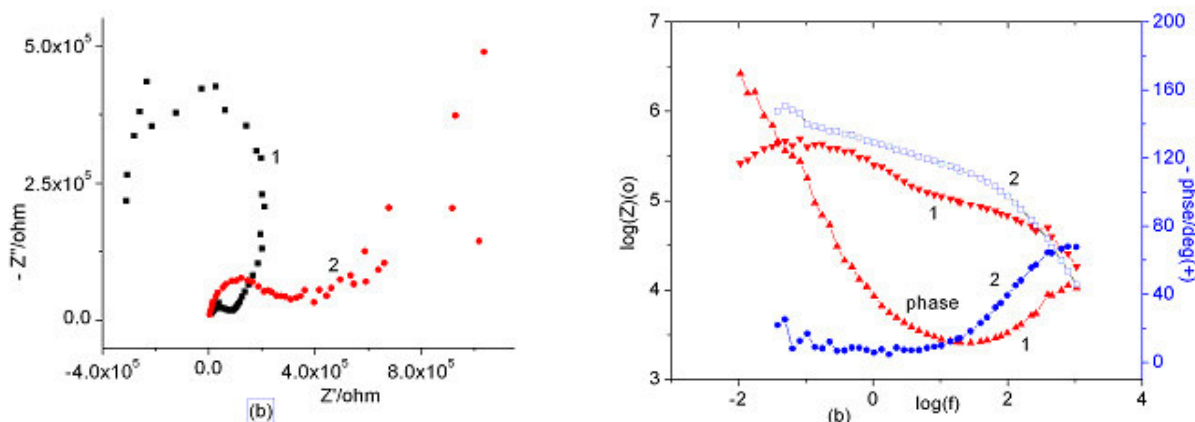
Figure 14. Impedance plots at 0.38 V, 1000 Hz – 5 mHz for a) Nyquist plot, 1, 25 mg/mL prothrombin; 2, 25 mg/mL prothrombin in 0.10 M NaCl; b) Bode plot, 1, 25 mg/mL prothrombin; 2, 25 mg/mL prothrombin in 0.10 M NaCl

It is interesting to note that while NaCl impedes the self-assembly behavior of prothrombin it promotes the self-assembly of collagen [21].

3.3.7. Negative differential resistance

This kind of impedance behavior with negative differential resistance has been seen in a few systems with passivation of electrodes, and it has been suggested it is tunnel diode behavior or resonant tunneling. We have also observed such a behavior for DNA-H_2O_2-sodium acetate buffer

system [13]. Systems with impedance loci in four quadrants have also been observed [22-28] in electrode passivation studies. Nonequilibrium thermodynamics with saddle-node and hopf bifurcations have been utilized to explain these observations. Such passivation systems have been thought to explain dynamical spatio temporal phenomena and oscillations in biological systems. We have observed several examples of biological systems, for the first time, to have impedance loci in four quadrants [29]. Our present system, though not spectacular, is indicative of tunnel diode behavior or resonant tunneling. When the potential or concentration is not optimum, chaotic state of the oscillations is also indicated. The hump or shoulder in the second quadrant probably is indicative of the peculiarity of the two kringles in the structure of prothrombin. However without the data for thrombin, it is premature to emphasize its role.

Our impedance data with loci in the first two quadrants at anodic potentials seems to be characteristic of systems with liquid crystal behavior or self-assembly in solution. This reversal happens only at a narrow band of potential suggestive of semiconduction. At high concentrations of prothrombin the reversal process tolerates small amounts of NaCl. However increasing the concentration of NaCl at a lower concentration of prothrombin hinders the reversal process. This is in contrast to the behavior observed for DNA and it seems prothrombin signaling does not require the assistance of electrolytes.

The cyclic voltammetry data indicate definite adsorption even at 2.5 mg/mL and the nature of the adsorption is very similar to the higher concentrations. However the observed negative differential resistance is dominant at the higher concentrations and absent at lower concentrations. Thus it is evident that the passivation of the electrode as well as the adsorption of prothrombin cannot sufficiently explain the impedance data, especially the negative differential resistance. Therefore we have to assume that even under the present conditions where the mercury may be passivated, the self-assembly of the molecules in the double layer and in the bulk must play a significant role in contributing to the negative differential resistance. We believe the self-assembly of the molecules provides a spatial extension of the electrode to the bulk and provides a pathway for proton and or electron mobility. We also assume that the orientation of the water molecules on the surface of these biological molecules changes significantly at lower frequencies.

3.4. Passivation of mercury

Our admittance data shown in Figure 5 confirm the well known passivation behavior of mercury at positive potentials. It is also well known that mercury forms a film of Hg_2Cl_2 in the presence of chloride. Thus applications of positive potentials to mercury electrodes not only changes the charge on the surface but also results in the modification of the metal surface. We had shown earlier from studies of potassium halides that admittance measurements can definitely pinpoint the region of this interaction [30].

Information on solute-solvent interactions can be obtained by careful evaluation of admittance, Nyquist, and Bode plots. We now know that NaCl alone cannot produce negative differential resistance in the passivation region of mercury [30]. While NaCl facilitates the formation of negative differential resistance formation in the impedance curves for collagen [21] it impedes in the present

case with prothrombin. We also know that oxide formation on mercury surface is not sufficient enough to observe negative differential resistance because we do not observe any with low prothrombin concentrations of 2.5 mg/mL or lower. Thus our results strongly suggest the influence of the self-assembly behavior of prothrombin at concentrations greater than 2.5mg/mL on the oscillatory behavior of the system and consequent exhibition of negative differential resistance in impedance curves. We have also observed that exhibition of impedance curves with negative differential resistance is not dictated by the passivation of mercury alone but rather by the system conditions. For example, molybdate-peroxide system exhibits negative differential resistance anywhere in the range -1.0 to + 0.2V depending on the pH [31], at about -1.0V in basic solutions, at about -0.4 V in slightly acidic solutions, and at about 0.2 V at pH values less than 2 [32]. Molybdate-flavin adenine dinucleotide system exhibits negative differential resistance at about -0.8 V [31].

3.5. Differential Capacitance

When ohmic resistance is compensated, differential capacitance measurements yield double layer capacitance, C_{dl} or Cs. In such a case the Cs should be independent of frequency. The differential capacitance data shown in Figure 15a indicate some frequency dependent dispersion. Figure 15b compares the capacitance data of 25mg/mL prothrombin in the absence and presence of 0.10 M NaCl.
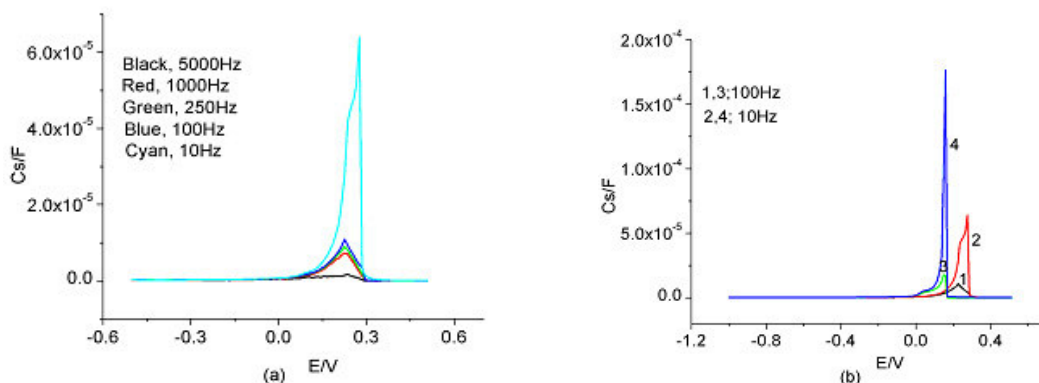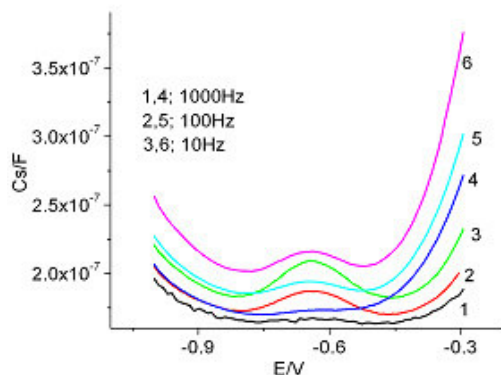

Figure 15. The capacitance data for a) 25 mg/mL prothrombin from bovine plasma b) comparison of capacitance; 1,2 prothrombin only (25mg/mL); 3,4, prothrombin (25mg/mL) in 0.10 M NaCl

The capacitance maximum is shifted slightly to more cathodic potentials in the presence of NaCl. We have observed dependence of differential capacitance for aqueous solutions of potassium halides [30]. Dispersion in differential capacitance observed for Ag(111) in 0.01 M NaCl [33] has been attributed to the real surface with fractal character instead of an ideal homogenous electrode surface. Our results are similar for 10 mg/mL prothrombin in 0.1M NaCl. The potential for the peak capacitance of prothrombin-NaCl mixture is in between that of NaCl and pure prothrombin. The capacitance values also follow the same trend.

The data in the cathodic potential range, in an expanded window are shown in Figure 16. It is remarkable that two capacitance minima are observed. This is somewhat similar to the behavior we have seen for the behavior of collagen in the presence and absence of NaCl [21]. However in the case

of collagen, the admittance data also gives clear cut evidence for these two minima. The admittance data for prothrombin are more difficult to plot on the same scale because of the much higher admittance in the presence of 0.10 M NaCl. However these data also demonstrate evidence for the present observations in capacitance characteristics. Another phenomenon we have noticed is that the first minimum seems to shift slightly more cathodic and the second minimum to slightly more anodic potentials with decrease in frequency. This behavior is the same both in the presence and absence of NaCl.

Figure 16. The capacitance data at cathodic potentials for 25 mg/mL prothrombin from bovine plasma 1, 1000 Hz; 2, 100 Hz; and 3, 10 Hz and 25 mg/mL prothrombin in 0.10 M NaCl, 4, 1000 Hz; 5, 100 Hz and 6, 10 Hz.

3.6. Semiconduction

The capacitance response (in the cathodic region) for a p-type semiconductor is often related to the inner layer of oxide. The capacitance response (in the anodic region) for an n-type semiconductor is related to characterize the outer layer of hydroxide. The concentrations of acceptors and donors in passive films can be calculated from the slopes of the linear sections of Mott-Schottky plots. For an n-type semiconductor,

$1/C^2 = 2/\varepsilon\varepsilon_o eN_D$ [E - E_{fb} – kT/e], and for a p-type semiconductor

$1/C^2 = - 2/\varepsilon\varepsilon_o eN_A$ [E-E_{fb} – kT/e]

where ε is the dielectric constant of the semiconductor, ε_o the vacuum permittivity, e the electron charge, N_D the donor density, N_A the acceptor density, E the applied potential, E_{fb} the flat-band potential, k the Boltzmann constant and T the absolute temperature. For the passive films in general, ε is about 40, εo is 8.854 x 10^{-12} Fm^{-1}, e is 1.6 x 10^{-19} C, and k is 1.38 x 10^{-23} JK^{-1}. The typical Mott-Schottky plot with 25 mg/mL prothrombin, and 25 mg/mL prothrombin in 0.10 M NaCl, are shown in Figure 17. To show that looks can often be deceiving, we have expanded the cathodic region and these plots are shown in Figure 18. These results suggest both p-type and n-type demiconduction for the
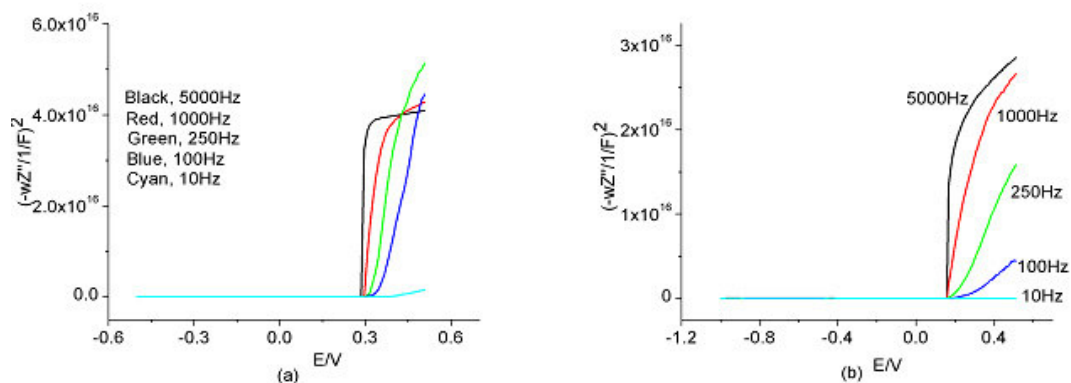
Figure 17. Mott-Schottky plots for a) 25 mg/mL prothrombin from bovine plasma and b) 25 mg/mL prothrombin in 0.10 M NaCl.
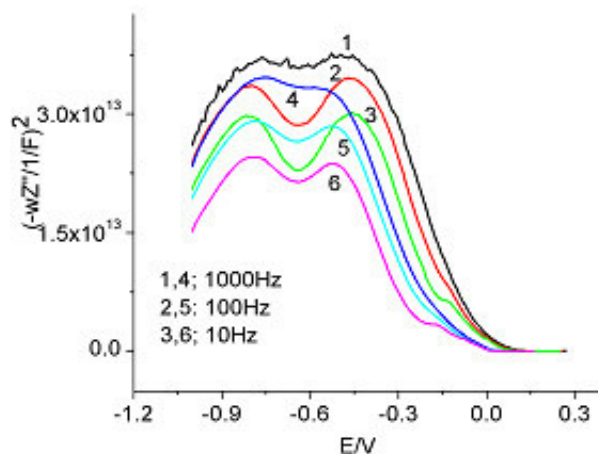

Figure 18. Mott-Schottky plot at cathodic potentials for 25 mg/mL prothrombin from bovine plasma 1, 1000 Hz; 2, 100 Hz; and 3, 10 Hz and 25 mg/mL prothrombin in 0.10 M NaCl, 4, 1000 Hz; 5, 100 Hz and 6, 10 Hz.

passive film formed on mercury and are similar to the behavior observed for alkali halides. It is possible the self-assembled molecules in solution provide a spatial extension of the electrode system into the bulk, contributing to the semi conduction behavior.

4. LIQUID CRYSTAL BEHAVIOR OR SELF-ASSEMBLY IN SOLUTIONS

The phase microscopy picture (300X) of 25 mg/mL prothrombin is shown in Figure 19a. The prothrombin picture demonstrates periodicity. This may contribute to the directional oscillation phenomenon in the impedance measurements associated with negative differential resistance. We could see the liquid crystal periodicity even at 2.5 mg/mL concentration, though not well defined compared to the higher concentration. We could not satisfactorily visualize any self-assembly of prothrombin, 25 g/mL in 0.1M NaCl. Instead we could see only broken fragments with occasional condensed fibers. This is consistent with the fact that we did not observe any impedance with this

system that exhibited negative differential resistance. The picture of prothrombin at the low concentration of 2.5 mg/mL in 0.1 M NaCl shown in Figure 19b shows ferns with global packing. On the other hand we could not see any clear picture of prothrombin in 0.005 M NaCl. Here again we observed broken fragments with some condensed fibers. Thus these pictures suggest that the self-assembly of prothrombin is concentration dependent. Also the nature of self-assembly is different in the presence of the electrolyte NaCl. The differences observed suggest that the self-assembly behavior is dependent both on the concentration of prothrombin as well as the electrolyte. It is known that the stimulation of prothrombin activation by positively charged membranes is suppressed at ionic strengths 0.10 or higher [17, 34]. Of course the role of calcium in blood coagulation is well established [17]. We plan to study the impedance characteristics of prothrombin in the presence of calcium ions,
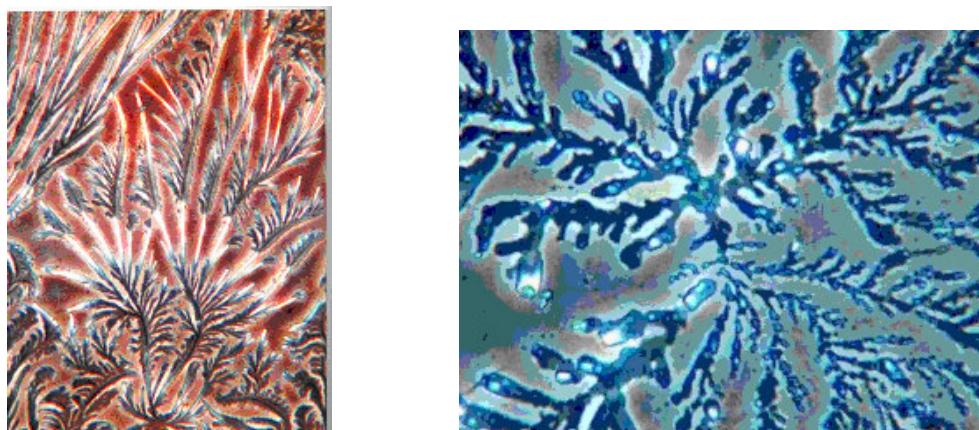
Figure 19. Phase microscopy (300X) of prothrombin from bovine plasma, pH 6.88 a) 25 mg/mL; b) 2.5 mg/mL in 0.10 M NaCl.

which we hope will further elucidate the influence of the charge.

The physics of nonequilibrium systems have been utilized to explain the pattern formation during self-organization of lubricating bacterial colonies shaped by diffusive instabilities [35]. Similar to the growth of the bacterial colonies our pictures exhibit branching patterns and random orientations within the branch. However it must be noted that the branch has a well defined envelope similar to the bacterial colonies [35].

5. CONCLUSIONS

Cyclic voltammograms of prothrombin indicate adsorption at the electrode and this adsorption is dependent on the concentration. There is a strong interaction of prothrombin with NaCl, and this shifts the potentials at which adsorption takes place. Admittance data indicate structure breaking and orientation effects of water at low frequencies when the potential of the mercury electrode changes slowly from negative to positive. Nyquist plots exhibit negative differential resistance and are indicative of resonant tunneling. A second hump in the impedance loci in the second quadrant suggests probable oscillation effects arising from the two kringle structures in prothrombin. At low

concentrations the impedance data show chaotic behavior, the last of the oscillatory process. Differential capacitance data exhibit dispersion, and Mott-Schottky plot indicates semiconduction. The presence of NaCl inhibits the resonant tunneling process. Phase microscopy of prothrombin shows unique periodicity in the self-assembly, suggesting oscillation between the branched and unbranched states.

References

1. B. Jayaram, T. Jain, *Annu. Rev. Biophys. Biomol. Struct.* 33 (2004) 343
2. M. Levitt, B.H. Park, *Structure,* 1 (1993) 223
3. W. Saenger, *Ann. Rev. Biophys. Biophys. Chem.,* 16 (1987) 93
4. W.H. Robertson, M.A. Johnson, *Ann. Rev. Phys. Chem.,* 54 (2003) 173
5. J.L. Finney, in: F. Franks (Ed.), *The Organization and Function of Water in Protein Crystals, in: Water, A Comprehensive Treatise,* vol.6, Recent Advances, Plenum Press, New York, 1979, Ch. 2.
6. A.A. Gardner, J.P. Valleau, J. Chem. Physics, 86 (1987) 4171
7. D. Marx, *Science,* 303 (2004) 634
8. S.K. Blau, *Physics Today*, March (2005) 21
9. C.V. Krishnan, M. Garnett, 1st Spring Meeting of the ISE, Spain, Abs. No. P06 (2003)
10. C.V. Krishnan, M. Garnett, 203rd Meeting of Electrochemical Society, Paris, Abs. No. 2703(2003)
11. C.V.Krishnan, M.Garnett, 204th Meeting of ECS, Orlando, Abs. No. 1378 (2003)
12. M. Garnett, C.V. Krishnan, 204th Meeting of Electrochemical Society, Orlando, Abs. No. 1377 (2003)
13. M.Garnett, C.V. Krishnan, 204th Meeting of ECS, Orlando, Florida, Abs. No. 1379 (2003)
14. D. Voet, J.G. Voet, Biochemistry, 2nd Ed., John Wiley & Sons, Inc., NY, p. 1205 (1995)
15. M. Garnett, J.L. Remo, 200th Meeting of ECS, San Francisco, Abs. No. 1132 (2001)
16. M. Garnett, C.V. Krishnan, 201st Meeting of ECS, Philadelphia, Abs. No. 78 (2002)
17. J. Rosing, G. Trans, H. Speijer, R.F.A. Zwaal, *Biochem.,* 27 (1988) 9048
18. L. Duic, S. Srinivasan, P.N. Sawyer, *J. Electrochem. Soc.,* 120 (1973) 348
19. A.J. Bard, L.R. Faulkner, Electrochemical Methods, John Wiley & Sons, Inc., 2nd Edition (2001) 599
20. H. Durliat, C. Davet, M. Comtat, *J. Electrochem. Soc., 132* (1985) 1594
21. C.V. Krishnan, M. Garnett, *Int. J. Electrochem. Sci.,* 1(2006) 215
22. P. Strasser, *The Electrochemical Society Interface,* Winter (2000) 46
23. M.T.M. Koper, *J. Chem. Soc. Faraday Trans., 94* (1998) 1369
24. A. Sadkowski, M. Dolata, J.P. Diard, *J. Electrochem. Soc., 151* (2004) E-20
25. A. Sadkowski, *J. Electroanal. Chemistry,* 573 (2004) 241
26. B. Miller, A. Chen, *Electrochim. Acta,* 50 (2005) 2203
27. M. Keddam, H. Takenouti, N. Yu, *J. Electrochem. Soc.,* 132 (1985) 2561
28. D.D. Macdonald, *Electrochim. Acta,* 35 (1990) 1509
29. C. V. Krishnan, Merrill Garnett, in *"Passivation of Metals and Semiconductors, and Properties of Thin Oxide Layers"*, P. Marcus and V. Maurice (Editors), Elsevier, Amsterdam, (2006) 389
30. C.V. Krishnan, M. Garnett, *Electrochimica Acta,* 51 (2006) 1541
31. C. V. Krishnan, Merrill Garnett, B. Chu, paper accepted, to be presented at the 210th Electrochemical Society Meeting, Cancun, Mexico (2006)
32. C. V. Krishnan, Merrill Garnett, B. Chu, 4th Spring Meeting of the International Society of Electrochemistry, Singapore, Abstract No. HC-O-23 (2006)

33. V. D. Jovic, B.M. Jovic, *J. Electroanal. Chem.,* 54 (2003) 1
34. C. M. Jackson, Y. Nemerson, *Ann. Rev. Biochem.,* 49 (1980) 765
35. H. Levine, E. Ben-Jacob, *Phys. Biol.,* 1 (2004) P14